

*Erik Jonsson School of Engineering and Computer Science
Texas Analog Center of Excellence*

Functional Performance of a Millimeter Wave Square Holey Dielectric Waveguide

UT Dallas Author(s):

Michael Gomez
C. Miller
Rashaunda Henderson
Kenneth K. O

Citation:

Aflakian, N., M. Gomez, C. Miller, R. Henderson, et al. 2019. "Functional Performance of a Millimeter Wave Square Holey Dielectric Waveguide." 2019 IEEE Radio and Wireless Symposium: 317-320, doi: 10.1109/RWS.2019.8714541

Copyright law restricts access to full text from Treasures @ UT Dallas to users with a valid UT Dallas NetID and password. Authorized users may click the link below to gain entry into the publisher's website.

<http://utd.edu/t/6152>

Functional Performance of a Millimeter Wave Square Holey Dielectric Waveguide

N. Aflakian¹, M. Gomez², C. Miller², R. Henderson², D. MacFarlane¹, K. K. O²

¹Electrical Engineering Dept., Southern Methodist University, Dallas, TX 75205

²Electrical and Computer Eng. Dept., The University of Texas at Dallas, Richardson, TX 75080

Abstract — This paper presents the functional performance of a square holey dielectric waveguide that operates from 180 to 360 GHz for supporting high data rate communication systems. A 7 cm waveguide is excited using a microstrip patch antenna at 264 GHz and shows 30 dB improvement from the system noise floor and 12 dB improvement from a free space transmission in an uncalibrated measurement. This waveguide minimizes cross talk and allows for polarization division multiplexing supporting vertical and horizontal polarizations.

Index Terms — dielectric waveguide, interconnect, millimeter wave.

I. INTRODUCTION

An all-electrical high data rate communication link has become an increasingly interesting research topic. High frequency data communication is approaching a bottleneck due to ohmic losses inherent in metallic interconnects [1, 2]. Optical interconnects could provide a solution to lower the loss, but they require efficient electro-optical conversion at transmitter and receiver ends. Dielectric THz waveguides have been developed for chip-to-chip communications using the native radiation of electronics. THz interconnects have lower loss compared to electric interconnects, and there is no need for electro-optical conversion. Dielectric waveguides presented for chip-to-chip applications usually have no cladding [3] or metallic cladding [4].

This paper presents the functional performance of a square dielectric holey cladding waveguide for chip-to-chip communication that operates from 180 to 360 GHz. Here, a cladding is provided for beam isolation to avoid bending or external perturbation losses, while preserving the waveguide flexibility. The square cross section of the waveguide allows for polarization division multiplexing (PDM) with minimal cross talk compared to conventional circular fibers. A planar patch antenna operating at 264 GHz has been used to excite the waveguide, which has been placed inside a horn antenna for two-port measurements. The patch antenna is a standalone device in this work but may be integrated onto a manufactured chip. Further improvements may be achieved using a coupling method to efficiently transfer the RF signal from the patch antenna to the dielectric waveguide.

II. SQUARE HOLEY DIELECTRIC WAVEGUIDE

A square holey dielectric waveguide was designed, fabricated, and tested [5]. The waveguide supports vertical and

horizontal states of polarization in the frequency range of 180 GHz to 360 GHz. Fig. 1 shows the 2 mm \times 2 mm square waveguide with eight 400 μ m holes in the cladding. Simulations, using Lumerical Mode Solutions software [6], show the output mode profile at 180 GHz for vertical and horizontal states of polarization. The square cross section allows the propagation of vertical and horizontal states of

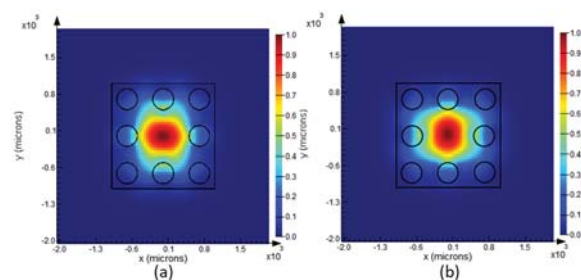


Fig. 1. Simulated holey cladding square waveguide at 180 GHz for (a) vertical and (b) horizontal polarization states.

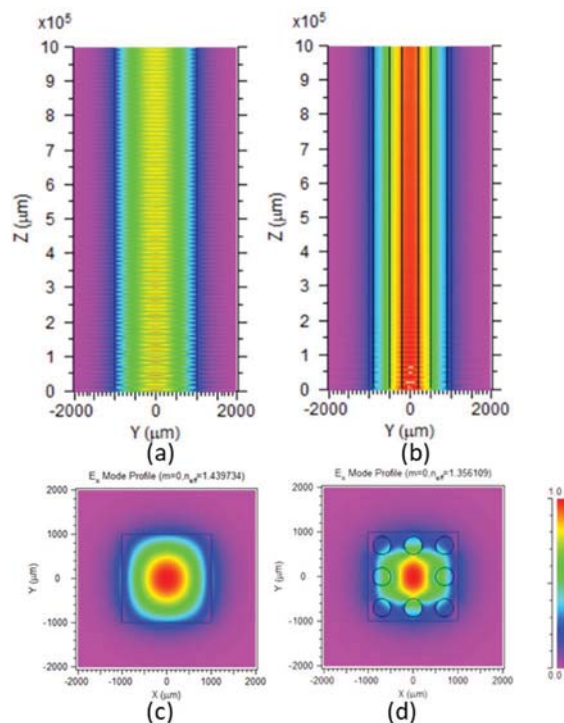


Fig. 2. Simulations of a waveguide in the (a), (c), absence and (b), (d) presence of holey cladding at 180 GHz.

polarization with minimum cross talk. The power coupling between the two states of polarization, simulated using Lumerical Mode Solutions software, was 0.00098 (-30 dB). The power coupling is defined as the simulated ratio of the total power coupled into a vertical polarization for a launched horizontal polarization beam (based on results in Fig. 1). The holey cladding creates a graded refractive index to isolate and protect the beam from external perturbation. A holey cladding is mostly beneficial at higher wavelengths in a broadband transmission. Fig. 2 shows the beam confinement at 180 GHz in the presence and absence of holey cladding, simulated using the Beam Prop software package of RSoft [7].

The cyclic olefin copolymer (COC) TOPAS (relative permittivity of 2.35 and loss tangent of 0.00002) was chosen for its low loss [8] of about 0.2dB/cm at 0.3 THz. The waveguide was fabricated using the three steps drill and draw technique used for porous optical fiber fabrications. The fabrication process is detailed in [5]. First, a 35 mm × 35 mm preform of raw TOPAS was molded. Next, eight holes were drilled into the preform. Then the preform shrinks into a 2 mm × 2 mm fiber by applying proper heat and pulling tension. Fig. 3 shows the cross section of a fabricated waveguide. We realized lengths of 15 cm to 200 cm. The performance of the waveguides has been demonstrated as indicated in [5] and [9].



Fig. 3. Composite image of fabricated waveguide cross section.

III. FUNCTIONAL CHARACTERIZATION

After verifying the modes of the waveguide and characterizing the loss from 220 to 320 GHz [9] we began functional performance testing by placing the waveguide in the vicinity of an antenna similar to the work in [10] and [11]. Fig 4 shows the experimental setup concept. A patch antenna is contacted using a ground-signal-ground (GSG) WR3 waveguide probe that is connected to a WR3 frequency extender module. An approximately 7 cm dielectric

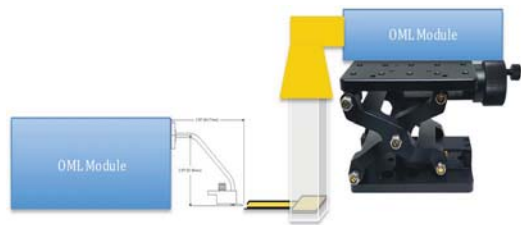


Fig. 4. Demonstration concept for exciting signal using on-wafer antenna and receiving it with the holey dielectric waveguide.

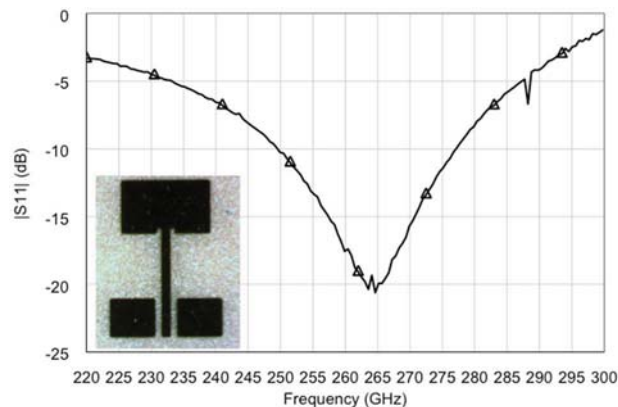


Fig. 5. Measured return loss of patch antenna used in the functional demonstration.

waveguide is placed above the antenna similar to other works. The dielectric waveguide is fed using the patch antenna and the output signal is coupled out using a WR3 horn antenna with 25 dB gain from MI-WAVE.

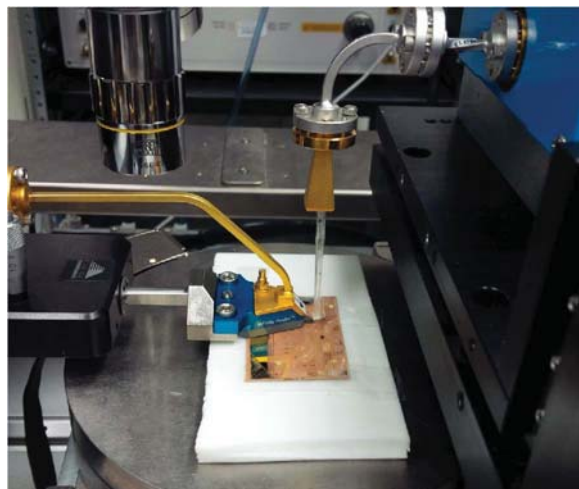


Fig. 6. Patch antenna on port 1 and horn antenna on port 2 with 7 cm holey waveguide placed above the horn antenna.

The microstrip inset fed patch antenna has dimensions of 0.386 mm × 0.277 mm with a conductor backed coplanar waveguide to microstrip transition for standalone probe characterization. The antenna is realized using photolithography steps and electron beam evaporation to provide a 0.5 micrometer thick gold metal layer using a 50 nanometer chromium adhesion layer. The dielectric material used is SU8 photoresist with relative permittivity of 3 and loss tangent of 0.04 at 200 GHz [12]. The antenna ground plane is realized using the top of a 0.125 mm thick FR408 substrate with 12 micrometers of copper metallization. An Agilent N5250A PNA with OML WR3 modules was used to measure the S_{11} of the antenna from 220 to 320 GHz after a short open load calibration. Fig. 5 shows the measured result with -20 dB $|S_{11}|$ at 264 GHz. The radiation pattern was also measured for

a similar antenna and showed a typical broad pattern with a 3dB beamwidth of approximately 60 degrees.

Fig. 6 shows the actual set up on the VNA where the antenna substrate is resting on a Rohacell® substrate above the metallized chuck. The dielectric waveguide is not directly touching the microstrip antenna. There is approximately a 2 mm air gap as seen in Fig. 7. The transmission $|S_{21}|$ was measured across the frequency range of 220 to 300 GHz. Two measurements were taken and are compared in Fig. 8. First the noise floor of the uncalibrated system is determined with no probe touching the antenna with the waveguide horn in position. This produces an average value of -60 dB across the range. The WR3 horn antenna is then included in the



Fig. 7. Side view showing waveguide is not directly touching the microstrip antenna and substrate. The patch radiates above the substrate and the field is coupled to the waveguide.

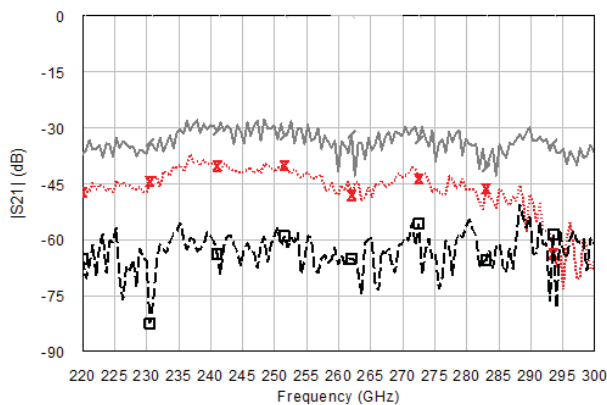


Fig. 8. Measured transmission loss for noise floor, horn antenna, horn and fiber together.

measurement and the antenna is contacted with the GSG probe. With the horn directly above the waveguide, the transmission signal increases to -45 dB across the band, despite that the antenna radiates at 264 GHz. Once the dielectric waveguide is included as shown in Fig. 6 and Fig. 7, the $|S_{21}|$, the transmission, increases an additional 12 dB to -33 dB. This indicates that the waveguide is capturing the signal similarly to the methods demonstrated in [9] and [10]. A transmission measurement with the dielectric waveguide and a

measurement in the absence of the dielectric waveguide produce a 12 dB difference. Note that this is a relative measurement to show waveguide effectiveness in transmission, the data does not represent absolute values. One of the challenges in this type of measurement is calibration, since one port is probe-based and the other is waveguide-based.

IV. CONCLUSION

A square holey cladding dielectric waveguide was presented as a chip-to-chip communication interconnect. The waveguide performance was tested using an antenna as the excitation source. The patch antenna, to be integrated on a chip ultimately, was used to feed the waveguide at 264 GHz. The waveguide was shown to increase the transmission by 12 dB compared to using only a horn antenna in a wireless configuration. Further improvements may be achieved using a coupling waveguide to increase the efficiency from the radiated antenna into the dielectric waveguide.

ACKNOWLEDGEMENT

This work is supported by Semiconductor Research Corporation (SRC) through Texas Analog Center of Excellence at the University of Texas at Dallas (Task ID 1836.156).

REFERENCES

- [1] S. Atakramians, S. Afshar V, T.M. Monro, and D. Abbott, "Terahertz dielectric waveguides," *Adv. Opt. Phot.* 5, 169–215 (2013).
- [2] B. Yu, et al., "High efficiency micromachined sub-thz channels for low-cost interconnect for planar integrated circuits," *IEEE Trans. Microw. Theory Techn.*, vol. 64, no. 1, pp. 96-105, Jan. 2016.
- [3] N. V. Thienen, Y. Zhang, M. D. Wit, and P. Reynaert "An 18 Gbps polymer microwave fiber (PMF) communication link in 40nm CMOS," *42nd Eu. S.-State Circ. Conf.*, pp. 483-486, (2016).
- [4] P. Reynaert, M. Tytgat, W. Volkaerts, A. Standaert, Y. Zhang, M.D. Wit, and N. V. Thienen, "Polymer microwave fibers: A blend of RF, copper and optical communication," *42nd Eu. S.-State Circ. Conf.*, pp. 15-20, (2016).
- [5] N. Aflakian, N. Yang, T. LaFave Jr, R. M. Henderson, K. K. O, and D. L. MacFarlane, "Square dielectric THz waveguides," *Opt. Exp.* 24, (13), 14951-14959 (2016).
- [6] <https://www.lumerical.com/tcad-products/mode/>
- [7] <https://www.synopsys.com/optical-solutions/rsoft/passive-device-beamprop.html>.
- [8] K. Nielsen, H. K. Rasmussen, A. J. L. Adam, P. C. M. Planken, O. Bang, and P. U. Jepsen, "Bendable, low-loss topas fibers for the terahertz frequency range," *Opt. Exp.*, vol. 17, pp. 8592-8601, (2009).
- [9] N. Aflakian, T. LaFave Jr, R. M. Henderson, K. K. O, and D. L. MacFarlane, "Square dielectric interconnect for chip-to-chip THz communication," *2017 Texas Symp. Wireless & MW. Circ. & Sys.* Waco, TX 2017, pp. 1-3.

- [10] S. Fukuda et al., "A 12.5+12.5 Gb/s full-duplex plastic waveguide interconnect," *IEEE Journal of Solid-State Circuits*, vol. 46, no. 12, pp. 3113-3125 (2011).
- [11] M. Tytgat, P. Reynaert, "A plastic waveguide receiver in 40nm CMOS with on-chip bondwire antenna," *2013 Proceedings of the ESSCIRC (ESSCIRC)*, Bucharest, 2013, pp. 335-338.
- [12] R. G. Pierce, R. Islam, R. M. Henderson, A. Blanchard, "SU-8 2000 millimeter wave material characterization," *IEEE Microwave and Wireless Components Letters*, vol. 24, no. 6, pp. 427-429, June 2014.